JOURNAL OF APPLIED ELECTROCHEMISTRY **16** (1986) 53–61

The effects of nickel and cobalt and their interaction with antimony on zinc electrowinning from industrial acid sulphate electrolyte

D. J. MACKINNON, R. M. MORRISON, J. M. BRANNEN

Metallurgical Chemistry Section, Mineral Sciences Laboratories, Canmet, Energy, Mines and Resources Canada, 555 Booth Street, Ottawa, Ontario K1A OG1, Canada

Received 24 December 1984

The effects of nickel and cobalt and their interaction with antimony on the electrowinning of zinc from industrial acid sulphate electrolyte were studied using X-ray diffraction, scanning electron microscopy and cyclic voltammetry. Concentrations of cobalt as high as 20 mg l^{-1} had no effect on the zinc deposition current efficiency. The current efficiency decreased rapidly when the electrolyte contained > 5 mg l^{-1} nickel. Neither cobalt or nickel had an effect on the morphology of the 1-h zinc deposits. Nickel and cobalt caused characteristic changes in the cyclic voltammograms for zinc deposition. As a result this technique might provide a rapid means for evaluating the electrolyte prior to zinc electrowinning. The combined presence of cobalt and antimony in the zinc electrolyte was more deleterious to zinc electrowinning than was the combined presence of nickel and antimony. The presence of 0.08 mg l^{-1} antimony in the electrolyte counteracted the effect of nickel both on the current efficiency for 1-h deposits and on the zinc deposition polarization curves.

1. Introduction

The presence of impurities in the electrolyte is a major problem for the zinc electrowinning industry. Decreases in zinc current efficiency and changes in deposit morphology and cathodic polarization occur for electrolytes containing small concentrations of impurities. Recent basic studies on zinc electrolysis [1–6] have shown a definite correlation between the zinc deposit morphology and the type and concentration of additives and/or impurities present in the electrolyte. Apart from producing characteristic morphology changes in zinc deposits, the various additives and impurities also affect the polarization curves for zinc deposition in a characteristic manner [2, 3]. As a result, it is possible to associate a given deposit morphology with a particular polarization (or overpotential) condition.

Antimony, which is one of the more harmful impurities contained in zinc electrolyte, was found to produce a characteristic type of zinc crystal growth consisting of large, poorly defined zinc platelets having a predominant [0 0 2] preferred orientation [1, 3]. Both glue and lead (Pb) were found to modify strongly zinc crystal growth by reducing the grain size and by changing the preferred orientation to [1 0 1] or [1 1 0] depending on their concentrations in the electrolyte [1, 3, 5]. Cadmium did not have an effect on the growth or orientation of the zinc deposit but did reduce the grain size [6].

Cobalt and nickel, impurities which are difficult to remove from the electrolyte, can have disastrous effects on zinc electrowinning under certain conditions which have yet to be clearly defined. Previous workers [7–9] have shown that an induction period of > 1 h exists before cobalt and nickel begin to have an effect on zinc deposition current efficiency. After the induction period the current efficiency decreases rapidly with time. The length of the induction period decreases with increasing temperature, increasing acid concentration and with decreasing current density. The behaviour of cobalt and nickel,

0021–891X/86 $03.00 + .12

which cause severe re-solution of the zinc deposit, has been interpreted in terms of the formation of local Zn–Co and Zn–Ni galvanic cells [10, 11]. Both cobalt [10] and nickel [12] were found to produce characteristic changes in the zinc deposition polarization curves. A nickel-activated hydrogen evolution peak was found to occur at low current densities during the anodic sweep portion of the cyclic voltammogram, the height of which was proportional to the nickel concentration in solution [12].

The present study was undertaken to examine the effects of cobalt and nickel and their interaction with antimony on the early stages of zinc deposition. The effects of these impurities on the current efficiency for zinc deposition and on the morphology and orientation of 1-h zinc deposits electrowon from industrial acid sulphate electrolyte under conditions normally applied in the zinc industry were determined. Cyclic voltammetry experiments were conducted to characterize the effects of nickel and cobalt in both the presence and absence of antimony on zinc deposition polarization.

2. Experimental details

2.1. *Electrolyte and apparatus*

The electrolyte was an industrial zinc sulphate solution prepared from hot zinc dust purified neutral zinc electrolyte obtained from Comico Ltd (Trail, British Columbia). The average analysis was in $g\,l^{-1}$: Zn 150, $MgSO_4$ 38, Mn 1.6; in $mg\,l^{-1}$: Cd 0.2, Sb 0.02, Co 0.3, Ge 0.01, Ni 0.1, Cu 0.1, Fe 0.9, Pb 0.2, Cl 80, F 3.

Cell solutions were prepared by adding H_2SO_4, redistilled water and impurities to the electrolyte to give final concentrations of $55\,g\,l^{-1}$ zinc and $150\,g\,l^{-1}$ H_2SO_4. Nickel and cobalt were added as sulphate solutions. Antimony additions were made as a potassium–antimony tartrate solution.

The electrolysis cell consisted of a $1\,dm^3$ beaker fitted with a Lucite cover which had slots cut in it to mount the electrodes [3]. A three-electrode assemblage consisting of a central aluminium cathode and two platinum anodes was used. The cathode was fashioned from 4.7 mm thick aluminium sheet (purity 99.6%) obtained from Cominco. It measured 31.8 × 136.3 mm. (The cathode was mounted so that zinc deposited on both sides onto a total area of $12.9\,cm^2$.) The anodes were cut from a 0.3 mm thick platinum sheet and measured 17.9 mm × 109.7 mm. The platinum anodes were used to avoid lead contamination of the electrolyte from conventional Pb–Ag anodes [5].

2.2. *Electrolysis*

The electrolysis was run in a constant temperature bath at 35° C with stirring at a cathode current density of $430\,A\,m^{-2}$ for a period of one hour.

2.3. *Examination of deposits*

Sections of the zinc deposits were examined by scanning electron microscopy to determine the surface morphology of the deposit and by X-ray diffraction to determine the preferred crystal orientation relative to the ASTM standard for zinc powder.

2.4. *Cyclic voltammetry*

Cyclic voltammograms were obtained using a voltage scan generator, a potentiostat and a x–y recorder for recording current versus applied potential plots. The voltage scan generator was used to cycle the potential from -0.85 to about -1.12 V versus a saturated calomel electrode. The latter limit being determined to give a maximum current of approximately 65 mA on the forward scan; hence, there is some variation in the potential scan rate. The scan was operated at a rate of $1\,mV\,s^{-1}$.

The same cell was used for both the cyclic voltammetry and the electrowinning, but the electrode assemblies differed. The working electrode was an aluminium cathode measuring 15.4 mm by 109.5 mm by 0.8 mm thick. It was mounted so that the surface area was approximately $3.2\,cm^2$. The counter electrode was one of the platinum anodes used in electrowinning. A saturated calomel electrode mounted adjacent to the cathode was used as the reference electrode.

Prior to each test the cathode was conditioned by polishing with 600 grit paper, washing with

acetone followed by redistilled water, and patting the cathode dry with a tissue. The cathode was then put into the cell while the electrolyte was stirred. Once a steady rest potential was established, the stirrer was turned off and the scan was initiated.

3. Results and discussion

3.1. *Current efficiency*

The effect of increasing concentrations of cobalt and nickel on the current efficiency (*CE*) for 1-h zinc deposits electrowon at $430\,A\,m^{-2}$ from industrial acid sulphate electrolyte is shown in Figs 1 and 2. The *CE* remained $\geqslant 90\%$ for cobalt concentrations $\leqslant 10\,mg\,l^{-1}$, Fig. 1; at $20\,mg\,l^{-1}$ cobalt, the *CE* decreased to 81%.

The presence of nickel in the electrolyte had a more detrimental effect than cobalt on the *CE* as indicated in Fig. 2. For nickel concentrations $> 5\,mg\,l^{-1}$, the *CE* decreased rapidly; it decreased to 25% for $10\,mg\,l^{-1}$ nickel and to 0% for $20\,mg\,l^{-1}$ nickel.

Interactions among impurities are important particularly because impurities which do not exhibit an effect when present alone can become intolerable when small amounts of another impurity are introduced. Antimony is frequently added to the electrolyte in small concentrations with glue in order to control deposit growth [1]. The effect of $0.08\,mg\,l^{-1}$ antimony in combination with increasing concentrations of cobalt and nickel on the *CE* for 1-h zinc deposits is also shown in Figs 1 and 2. At $0\,mg\,l^{-1}$ cobalt or nickel, the addition of $0.08\,mg\,l^{-1}$ antimony to the electrolyte resulted in a decrease in *CE* from 92 to 74%. For cobalt concentrations $> 5\,mg\,l^{-1}$ the *CE* decreased rapidly, falling to a value of 8% at $20\,mg\,l^{-1}$ cobalt, Fig. 1.

Increasing concentrations of nickel in the presence of $0.08\,mg\,l^{-1}$ antimony caused only a small decrease in the *CE*; for $20\,mg\,l^{-1}$ nickel, the *CE* was reduced from 74 to 69%, Fig. 2. Thus, for nickel concentrations $> 5\,mg\,l^{-1}$ the presence of $0.08\,mg\,l^{-1}$ antimony in the electrolyte had a beneficial effect on the *CE*; for $10\,mg\,l^{-1}$ nickel the *CE* increased from 25 to 70% and for $20\,mg\,l^{-1}$ nickel it increased from 8 to 69%.

3.2. *Deposit morphology and orientation*

The addition of $10\,mg\,l^{-1}$ nickel or $5\,mg\,l^{-1}$ cobalt to purified industrial acid sulphate electrolyte had no significant effect on either the zinc deposit morphology or the preferred orientation which were similar to those obtained from electrolyte containing no added impurities [3], Fig. 3. Fig. 3a shows the typical zinc deposit morphology obtained from purified industrial acid sulphate electrolyte. Fig. 3b and 3c show that similar morphologies were obtained when the electrolyte contained either $5\,mg\,l^{-1}$ cobalt or $10\,mg\,l^{-1}$ nickel. Increasing the cobalt concentration to $20\,mg\,l^{-1}$ did not change the preferred orientation nor the morphology of the 1-h zinc deposits, but concentrations of nickel

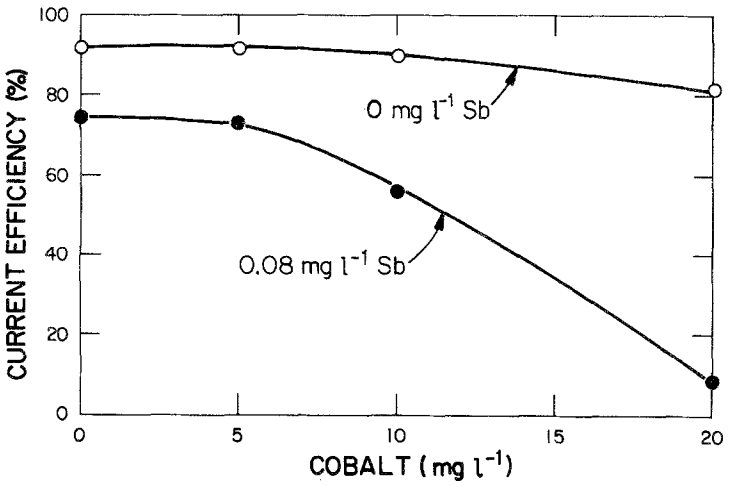

Fig. 1. Plots showing the effect of cobalt in the presence and absence of antimony on the current efficiency for 1-h zinc deposits electrowon at $430\,A\,m^{-2}$ from industrial acid sulphate electrolyte.

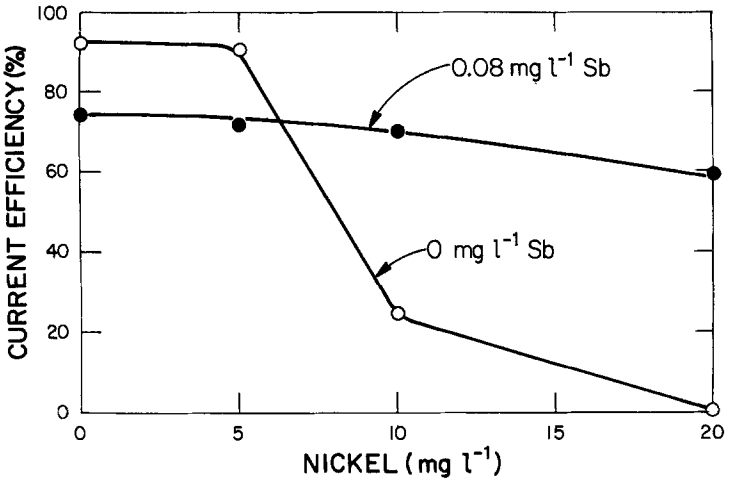

Fig. 2. Plots showing the effect of nickel in the presence and absence of antimony on the current efficiency for 1-h zinc deposits electrowon at 430 A m^{-2} from industrial acid sulphate electrolyte.

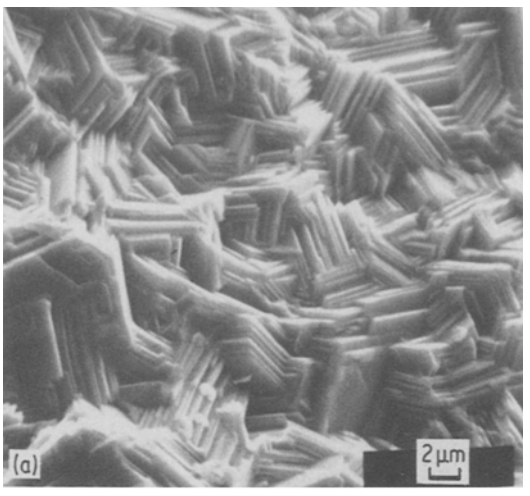

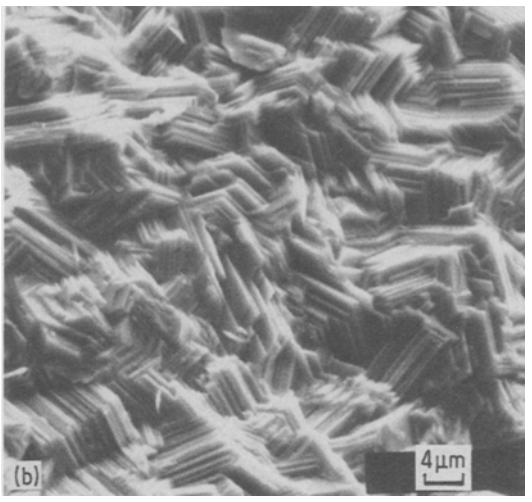

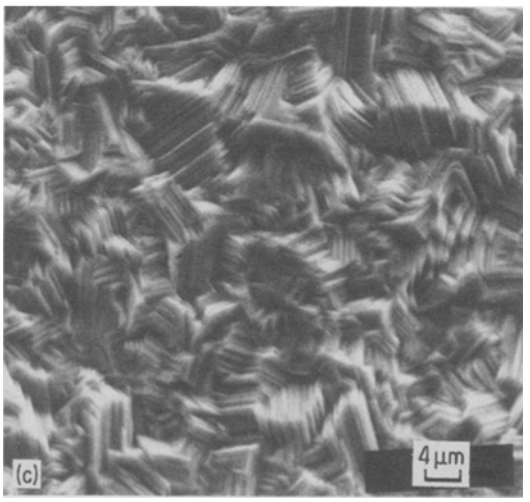

Fig. 3. SEM photomicrographs showing (a) the typical morphology of a 1-h zinc deposit electrowon at 430 A m^{-2} from purified industrial acid sulphate electrolyte; (b) the effect of 5 mg l^{-1} cobalt and (c) the effect of 10 mg l^{-1} nickel. Orientation [1 1 4] [1 0 2] [1 1 2].

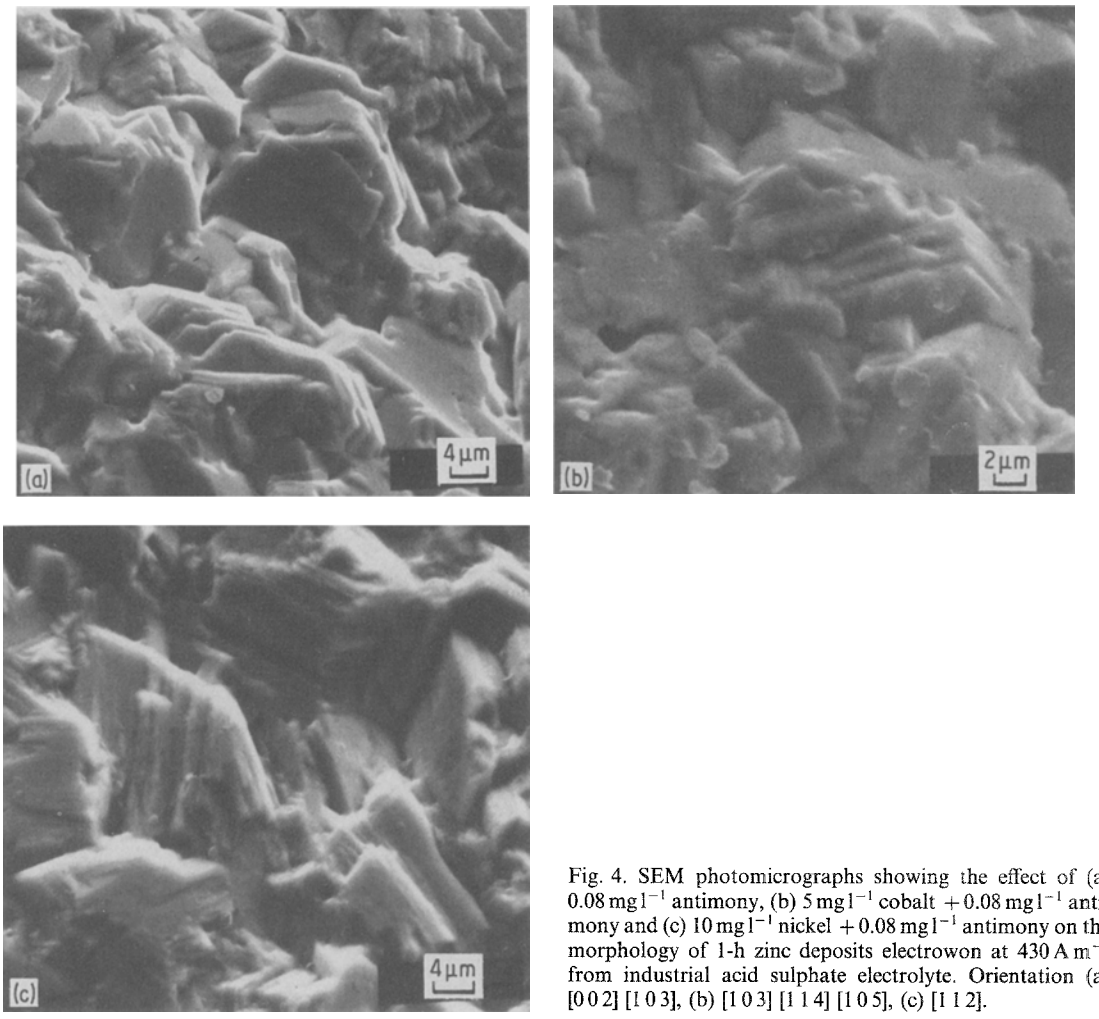

Fig. 4. SEM photomicrographs showing the effect of (a) 0.08 mg l^{-1} antimony, (b) 5 mg l^{-1} cobalt + 0.08 mg l^{-1} antimony and (c) 10 mg l^{-1} nickel + 0.08 mg l^{-1} antimony on the morphology of 1-h zinc deposits electrowon at 430 A m^{-2} from industrial acid sulphate electrolyte. Orientation (a) [0 0 2] [1 0 3], (b) [1 0 3] [1 1 4] [1 0 5], (c) [1 1 2].

> 10 mg l^{-1} reduced the deposit grain size; at 20 mg l^{-1} nickel, after 1-h electrolysis time, the zinc deposit was completely dissolved; i.e. $CE = 0\%$.

The effect of 0.08 mg l^{-1} antimony on the morphology of the 1-h zinc deposit is shown in Fig. 4a. The deposit consists of large, rounded platelets, having a preferred [0 0 2] [1 0 3] orientation. Such deposits are very susceptible to re-solution at crystal boundaries as zinc deposition progresses.

The addition of 5 mg l^{-1} cobalt to an electrolyte containing 0.08 mg l^{-1} antimony had no significant effect on the zinc deposit morphology, cf. Fig. 4a and b. The preferred orientation changed from [0 0 2] [1 0 3] to [1 0 3] [1 1 4] [1 0 5]. At cobalt concentrations > 5 mg l^{-1}, the preferred orientation reverted to [0 0 2] and the deposits showed substantial re-solution in agreement with the significant decrease in *CE* which occurred under these conditions, Fig. 1.

The addition of 10 mg l^{-1} nickel to an electrolyte containing 0.08 mg l^{-1} antimony changed the preferred orientation of the deposit from [0 0 2] to [1 1 2], similar to that obtained from addition-free electrolytes and from electrolytes containing cobalt or nickel but no antimony. The deposit morphology, however, still consisted of large, poorly defined platelets, similar to those obtained from an electrolyte containing antimony (see Fig. 4a), but in this case the platelets were aligned at intermediate angles to the cathode, Fig. 4c. This morphology and preferred orientation persisted for nickel concentrations

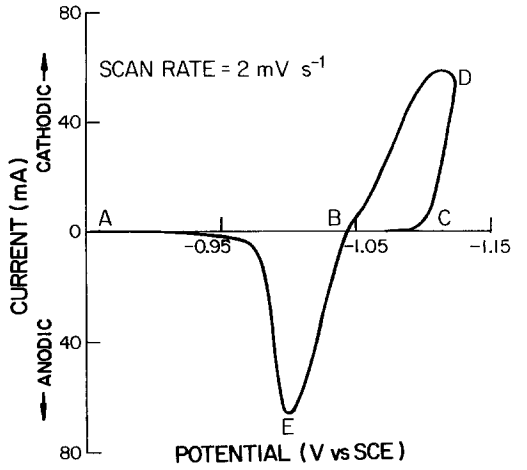

Fig. 5. Characteristic cyclic voltammogram obtained for purified industrial acid zinc sulphate electrolyte. Scan rate $= 2\,\text{mV}\,\text{s}^{-1}$.

to $20\,\text{mg}\,\text{l}^{-1}$ and as mentioned earlier the *CE* remained around 70% (see Fig. 2).

Thus, whereas the presence of nickel in the electrolyte appears to be more detrimental to zinc deposition than cobalt, the addition of $0.08\,\text{mg}\,\text{l}^{-1}$ antimony seems to reverse this trend. In order to establish the fundamental behaviour of these chemical species in the zinc electrolyte and of the zinc deposition process itself, the characteristic polarization curves for zinc deposition, in the presence and absence of these impurities, were obtained using cyclic voltammetry.

3.3. *Polarization effects*

The typical cyclic voltammogram obtained for purified industrial acid zinc sulphate electrolyte is shown in Fig. 5. A cycle starting from Point A (-0.85 V versus SCE) goes through a region of low current until Point C where zinc deposition commences. The current increases to Point D where the scan is reversed. The current then decreases, reaches zero at Point B where it becomes anodic corresponding to the dissolution of deposited zinc. The anodic peak is reached at E and dissolution is complete on return to A.

The effect of various concentrations of nickel

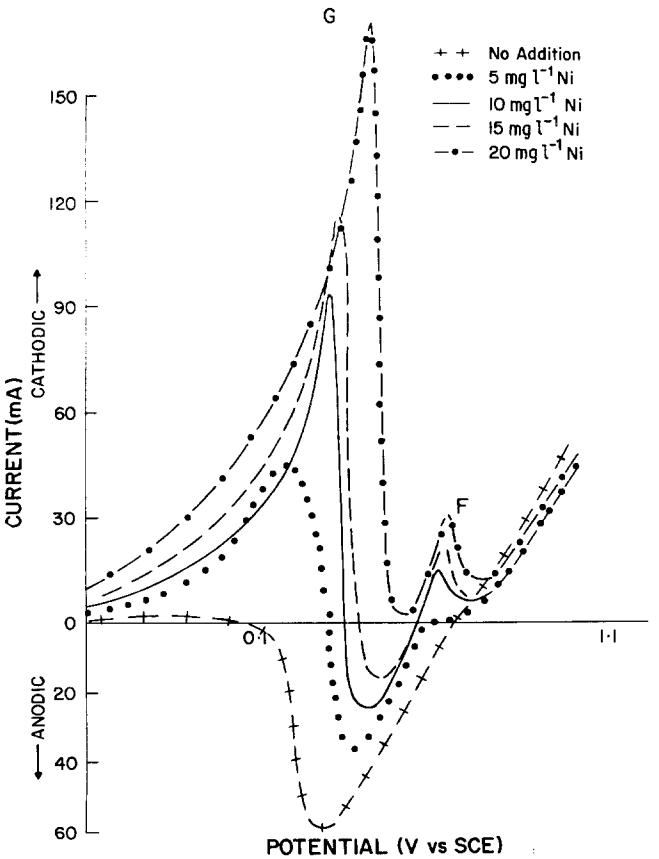

Fig. 6. Cyclic voltammograms showing the effect of nickel on zinc deposition polarization. Scan rate $= 1\,\text{mV}\,\text{s}^{-1}$.

on the cyclic voltammograms is shown in Fig. 6. Nickel had little effect on the front scan; i.e. the ACD portion of the voltammogram, so only the back or reverse scan portions of the voltammograms are highlighted. For nickel the reverse scan portion of the voltammograms was characterized by two cathodic peaks, one (Peak F) prior to the zero current line; i.e. while the current was still cathodic and one (Peak G) after the anodic dissolution of zinc was complete. Both peaks increased with increasing nickel concentration but Peak G was much more sensitive to the nickel concentration than Peak F.

Peak F, Fig. 6, is similar to that observed for industrial acid sulphate electrolyte containing germanium [13]. In that case, as well as in the present situation, Peak F was associated with vigorous hydrogen evolution. The presence of Peak F in the voltammogram was accompanied by a reduction in the corresponding anodic current peak, indicating that some of the deposited zinc had dissolved prior to the current becoming anodic. This behaviour suggests that a local cell-type impurity interaction occurs in the potential region of Peak F whereby nickel sites act as local cathodes and the adjacent zinc sites as local anodes [10–13].

With reference to Fig. 6, for 20 mg l^{-1} nickel, the anodic peak for zinc dissolution does not occur indicating that all zinc deposited prior to Peak F is completely dissolved from the cathode while the potential is in the region of Peak F. It will be recalled that, for the 1-h electrolysis test involving 20 mg l^{-1} nickel, the *CE* was 0% and a zinc deposit was not obtained.

Peak G, Fig. 6, occurred only after all the zinc had been dissolved from the cathode; i.e. after the anodic portion of the voltammogram. This peak, which is also associated with vigorous hydrogen evolution, indicates that nickel must remain on the cathode surface after zinc dissolution. A plot of peak height (G) versus nickel concentration, Fig. 7, indicates a linear relationship which might be useful as a means for rapidly detecting low levels of nickel in zinc electrolyte.

Fig. 8 compares the reverse scan portions of the voltammograms obtained from an electrolyte containing 10 mg l^{-1} nickel with those obtained from electrolytes containing 10 mg l^{-1} nickel with various concentrations (0.05 to 0.20 mg l^{-1})

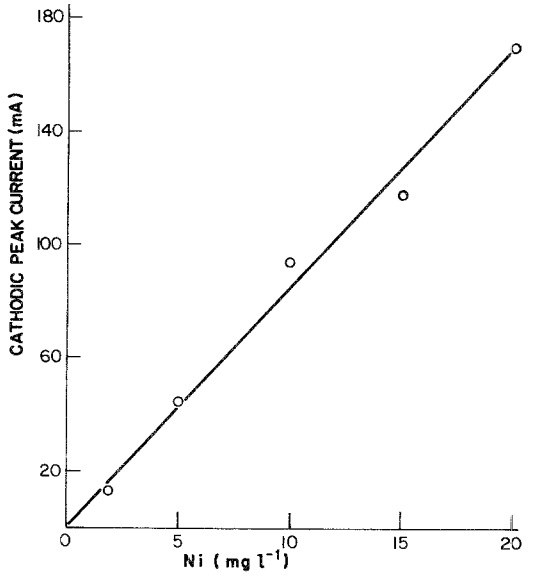

Fig. 7. Plot of cathodic peak current (G from Fig. 6) versus nickel concentration.

of antimony. The forward scans are all similar to Fig. 5 and again have not been included. While Peak F is slightly reduced, peak G is significantly reduced with the addition of 0.05 mg l^{-1} antimony. Higher antimony concentrations result in a further, less dramatic reduction in peak height (G). This result indicates that when antimony is present in the electrolyte, hydrogen evolution is inhibited and hence zinc deposit re-solution is lessened. This is in agreement with the *CE* results presented earlier which showed that in the presence of 0.08 mg l^{-1} antimony the *CE* remained at about 70% when the nickel concentration was increased to 20 mg l^{-1}, Fig. 2.

The effects of cobalt on the cyclic voltammogran for zinc were less pronounced than those of nickel. Fig. 9 compares the voltammograms obtained from electrolytes containing, 0, 9 and 27 mg l^{-1} cobalt. Increasing concentrations of cobalt had a slight effect on the forward scan indicating a small degree of depolarization.

At high cobalt concentration the reverse scan featured a broad shoulder prior to the crossover potential. Vigorous hydrogen evolution was observed to occur in this potential region. This was accompanied by simultaneous zinc re-solution as indicated by the substantial reduction in the anodic peak for zinc dissolution, Fig. 9.

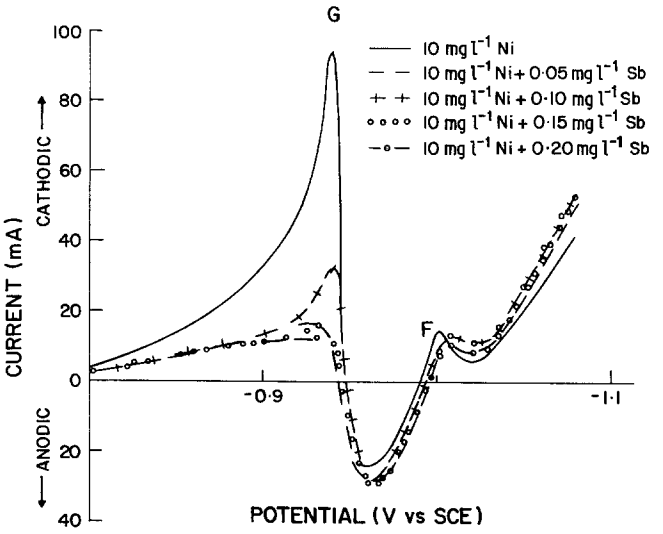

Fig. 8. Cyclic voltammograms showing the effect of nickel and nickel + antimony on zinc deposition polarization. Scan rate = 1 mV s^{-1}.

As was the case for nickel, a cathodic peak due to hydrogen evolution was observed after the zinc had been completely dissolved from the cathode, indicating that cobalt must remain on the cathode surface. The peak, however, was less sensitive than the corresponding nickel peak, indicating, in agreement with previous work [14], that at the same concentration level, nickel deposits with zinc to a greater extent than does cobalt.

Fig. 10 compares the voltammogram obtained for an electrolyte containing 10 mg l^{-1} cobalt with those obtained from electrolytes containing 10 mg l^{-1} cobalt and various concentrations (0.05 to 0.20 mg l^{-1}) of antimony. The combined presence of cobalt and antimony in the electrolyte at the levels indicated in Fig. 10 produced essentially an antimony-type voltammogram [2, 3]. This is in agreement with the antimony-type morphology (Fig. 4b) which was obtained for the 1-h deposits electrowon from solutions containing these concentrations of cobalt and antimony.

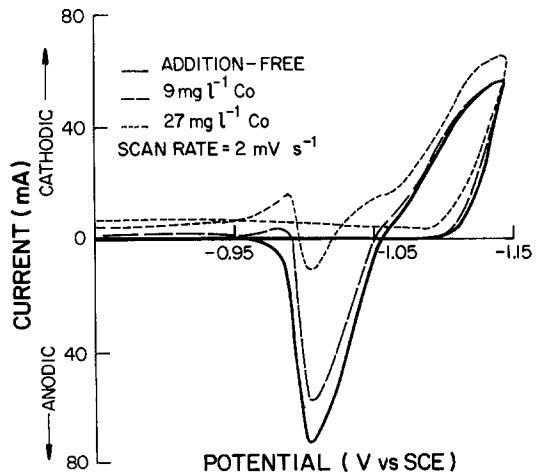

Fig. 9. Cyclic voltammograms showing the effect of cobalt on zinc deposition polarization. Scan rate = 2 mV s^{-1}.

4. Conclusions

The effects of nickel and cobalt and their interaction with antimony on zinc deposition current efficiency and polarization behaviour and on the morphology and orientation of 1-h zinc deposits electrowon from industrial acid zinc sulphate electrolyte have been determined. Although both nickel and cobalt had similar effects on the zinc deposit morphology and orientation, the presence of nickel in the electrolyte had a more deleterious effect than did cobalt on zinc deposition *CE* and consequently on deposit re-solution. Also, zinc deposition polarization curves were more sensitive to nickel than to cobalt in the electrolyte. The effects of nickel and cobalt on zinc electrowinning are consistent with a mechanism involving the formation of local cells whereby electrodeposited nickel or cobalt act as local cathodes for hydrogen evolution while adjacent zinc sites become local anodes for zinc dissolution. The combined presence of cobalt and antimony in the electrolyte was more deleterious to zinc electrowinning than the combined presence of nickel and antimony.

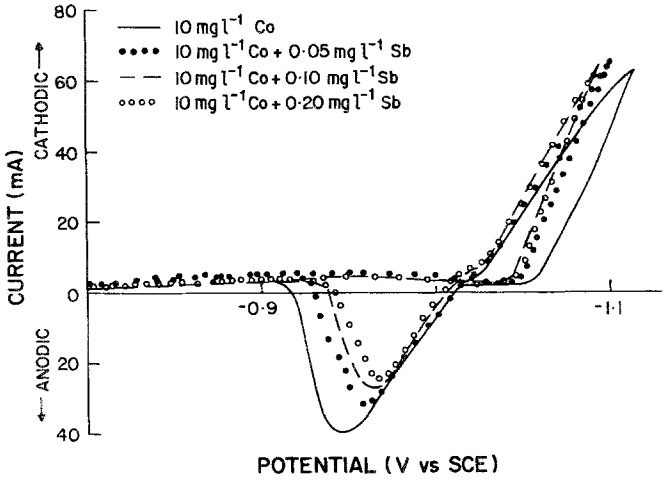

Fig. 10. Cyclic voltammograms showing the effect of cobalt and cobalt + antimony on zinc deposition polarization. Scan rate $= 1\,mV\,s^{-1}$.

Acknowledgements

Thanks are due to Cominco Ltd. for supplying the electrolyte and aluminium cathode sheet. D. Owens, Canmet, did the scanning electron microscopy on the zinc deposits and E. J. Murray and P. Carriere, Canmet, did the X-ray diffraction measurements.

References

[1] D. J. Robinson and T. J. O'Keefe, *J. Appl. Electrochem.* **6** (1976) 1.
[2] B. A. Lamping and T. J. O'Keefe, *Metall. Trans.* **7B** (1976) 551.
[3] D. J. MacKinnon and J. M. Brannen, *J. Appl. Electrochem.* **7** (1977) 451.
[4] R. C. Kerby, H. E. Jackson and T. J. O'Keefe, *Metall. Trans.* **8B** (1977) 661.
[5] D. J. MacKinnon, J. M. Brannen and R. C. Kerby, *J. Appl. Electrochem.* **9** (1979) 55.
[6] *Idem, ibid.* **9** (1979) 71.
[7] M. Maja and P. Spinelli, *J. Electrochem. Soc.* **118** (1971) 1538.
[8] I. W. Wark, *J. Appl. Electrochem.* **9** (1979) 721.
[9] M. Maja, N. Penazzi, R. Fratesi and G. Roventi, *J. Electrochem. Soc.* **129** (1982) 2695.
[10] D. R. Fosnacht and T. J. O'Keefe, *J. Appl. Electrochem.* **10** (1980) 495.
[11] R. Fratesi, G. Roventi, M. Maja and N. Penazzi, *ibid.* **10** (1980) 765.
[12] Yar-Ming Wang, T. J. O'Keefe and W. J. James, *J. Electrochem. Sco.* **127** (1980) 2589.
[13] D. J. MacKinnon and P. L. Fenn, *J. Appl. Electrochem.* **14** (1984) 467.
[14] R. Liebscher, *Neue Hutte* **14** (1969) 651.